

miR-4443 Contained Extracellular Vesicles: A Factor for Endometriosis Progression by PI3K/AKT/ACSS2 Cascade in-vitro

Sifan Ji^{1,2,*}, Hang Qi^{1,2,*}, Li Yan^{1,2,*}, Duo Zhang^{1,2}, Yang Wang^{1,2}, HaLiSai MuDanLiFu^{1,2}, Chuqing He^{1,2}, Wei Xia^{1,2}, Qian Zhu^{1,2}, Yan Liang^{1,2}, Jian Zhang^{1,2}

¹Department of Obstetrics and Gynecology, The International Peace Maternity and Child Health Hospital, School of Medicine, Shanghai Jiao Tong University, Shanghai, People's Republic of China; ²Shanghai Key Laboratory of Embryo Original Diseases, Shanghai, People's Republic of China

*These authors contributed equally to this work

Correspondence: Jian Zhang, Department of Obstetrics and Gynecology, The International Peace Maternity and Child Health Hospital, School of Medicine, Shanghai Jiao Tong University, Shanghai, People's Republic of China, Tel +86 18017316017, Email zhangjian_ipmch@sjtu.edu.cn

Introduction: Endometriosis (EM) is an estrogen-dependent benign gynecologic disease affecting approximately 10% of reproductive-age women with a high recurrence rate, but lacks reliable biomarkers. No previous studies have investigated the possible use of extracellular vesicle (EV)-associated micro RNAs (miRNAs) from menstrual blood (MB) as candidate diagnostic or prognostic markers of EM.

Methods: Specimens were obtained from endometriosis and non-endometriosis patients at the International Peace Maternity and Child Health Hospital in Shanghai. Microarray was used to screen differentially expressed miRNAs among peritoneal fluid (PF), fallopian tube fluid (FF), and MB. Dual-luciferase reporter gene assay was carried out to verify the relationship between miR-4443 and ACSS2. Cell proliferation and Transwell invasion assays were performed in vitro after intervention on miR-4443 and ACSS2 in hEM15A human endometrial stromal cells and primary human endometrial stromal cells (hESCs). Spearman correlation analysis, receiver operating characteristic (ROC) curve analysis, and survival analysis were applied to clinical data, including severity of symptoms and relapse of EM among EM patients.

Results: EV-associated miR-4443 was abundant in MB of endometriosis patients. ACSS2 knockdown and miR-4443 overexpression promoted cell proliferation and migration via the PI3K/AKT pathway. miR-4443 levels in MB-EVs were positively correlated with the degree of dyspareunia ($r=0.64$; $P<0.0001$) and dysmenorrhea ($r=0.42$; $P<0.01$) in the endometriosis group. ROC curve analyses showed an area under the curve (AUC) of 0.741 (95% CI 0.624–0.858; $P<0.05$) for miR-4443 and an AUC of 0.929 (95% CI 0.880–0.978; $P<0.05$) for the combination of miR-4443 and dysmenorrhea.

Conclusion: MB-derived EV-associated miR-4443 might participate in endometriosis development, thus providing a new candidate biomarker for the noninvasive prediction of endometriosis recurrence.

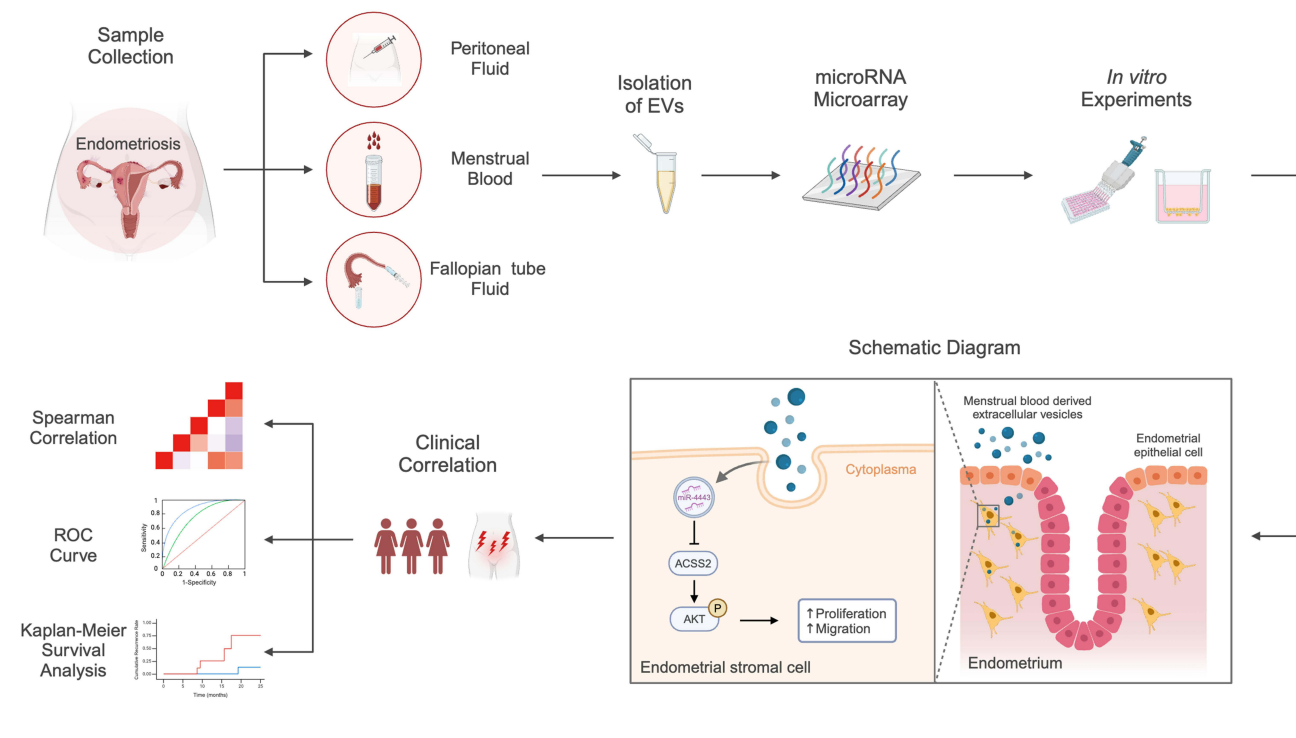
Keywords: endometriosis, menstrual blood, biomarker, extracellular vesicles, miR-4443

Introduction

Endometriosis (EM) is an estrogen-dependent benign gynecologic disease characterized by the growth and invasion of the uterine endometrium outside the uterine cavity.¹ Approximately 10% of reproductive-age women are diagnosed with EM, and 50% of EM patients suffer from chronic pelvic pain (CPP),^{1,2} which decreases the quality of life and affects the mental health of patients.^{3,4} Laparoscopic surgery remains the gold standard method for diagnosing and treating EM,⁵ but laparoscopic surgery is an invasive procedure that requires preparation and may have complications, and it is offered to selected patients.⁶ Therefore, finding noninvasive methods for the quick diagnosis and prediction of EM would be important.

The pathogenesis of EM and its recurrence are now considered much more complicated than that proposed by the “classic theory” which suggests that menstrual reflux leads to EM since EM occurs in only 10% of women with

Graphical Abstract



menstrual reflux.^{7,8} Deep EM, stage 3–4 EM, and time interval since surgery are risk factors for EM recurrence,⁹ while pregnancy after surgery is a protective factor.¹⁰

Menstrual blood (MB) contains a high concentration of endometrial cells, various cytokines, blood, peritoneal fluid (PF), and fallopian tube fluid (FF), reflecting dysregulation of the pelvic microenvironment of these patients.^{11,12} Furthermore, biomarkers in peripheral blood, such as CA125, have been widely applied in clinical work^{13–15} but are unreliable as diagnostic biomarkers for EM due to their low sensitivity and specificity.¹⁶ Thus, MB may harbor potential biomarkers that facilitate noninvasive diagnostic strategies for EM. miRNAs in extracellular vesicles (EVs) from peripheral blood or PF of EM patients can promote angiogenesis in human umbilical vein endothelial cells.¹⁷ Therefore, EVs miRNAs have been proposed as promising potential biomarkers for EM due to their high stability and specificity.¹⁶

In summary, this study aimed to isolate EV-encapsulated miRNAs from the MB of EM patients and investigate whether and how they could contribute to the pathogenesis of EM and whether they could be used to predict EM recurrence. EM patients were enrolled, and MB, FF, and PF were collected to screen for miRNA overlap among the three fluids. Then, the screened miRNAs were used in hEM15A human endometrial stromal cells and primary human endometrial stromal cells (hESCs) to determine their biological effects.

Materials and Methods

The Isolation and Examination of Extracellular Vesicles (EVs)

Menstrual blood (MB), peritoneal fluid (PF), and fallopian tube fluid (FF) samples were obtained from patients with endometriosis (case group) and patients without endometriosis (control group) with written informed consent. The collection method, inclusion and exclusion criteria, treatment methods, sample collection time, and preservation method are listed in the [Supplementary Methods](#) about ethical approval and sample collection.

As previously described, EVs were isolated from MB, PF, and FT by differential centrifugation and ultracentrifugation.¹⁸ Briefly, MB was centrifuged at 300 ×g for 10 min, then 2000 ×g for 10 min, and finally

ultracentrifuged at 100,000 $\times g$ for 2 h to remove the supernatant. The obtained pellet was re-suspended in PBS. Transmission electron microscopy (TEM; JEOL, Tokyo, Japan) of EVs was carried out using the uranyl acetate negative staining method. Nanoparticle-tracking analysis (NTA) was used to measure the diameters and concentrations of the EVs using ZetaVIEW S/N 17–310 (Particle Metrix, Meerbusch, Germany).

The Isolation and Culture of hESCs and hEM15A

hESCs from eutopic endometrial tissues were isolated and cultured as previously described, with some modifications.¹⁹ The hESCs from EM patients' eutopic endometrial tissues were EM-hESCs, and those from non-EM patients were NC-hESCs (non-EM hESCs). The human EM-derived immortalized endometrial stromal cell line hEM15A was provided by Dr. Xiaohong Chang (Peking University People's Hospital). The isolated cells were identified by immunofluorescence ([Supplementary Figure S1](#)). More details are described in the [Supplementary Methods](#) about isolation and culture of hESCs and hEM15A.

Retrovirus and Lentivirus Production and Construction of Stable Cell Lines

In order to establish stable cell lines, hEM15A cells and hESCs were transduced with retrovirus and lentivirus in the presence of 10 $\mu g/mL$ polybrene (Sigma, St. Louis, MI, USA). The procedure of retrovirus and lentivirus production is described in the [Supplementary Methods](#) about retrovirus and lentivirus production as well as construction of stable cell lines.

EVs Labeling and Internalization

EVs were labeled using the PKH67 Green Fluorescent Cell Linker Kits (Sigma, St. Louis, MI, USA) following the manufacturer's instructions. The internalization of EVs labeled with PKH67 in the human ESC cell line hEM15A and primary human endometrial stromal cells (hESCs) was analyzed following the manufacturer's instructions described in the [Supplementary Methods](#) about EVs labeling and internalization.

In vitro Cell Proliferation and Migration Assays

After transfection, hEM15A cells and hESCs were seeded on 96-well flat-bottomed microplates at a density of 6000 cells/well. The culture medium was regularly replaced. For the analysis of cell proliferation, 100 μL of Cell Counting Kit-8 (CCK-8) reagent (Yeasen, China) was added to each well at different time points (0, 24, 48, 72, and 96 h), followed by incubation for 1 h at 37°C. The absorbance of each well at 450 nm was observed and measured with a Universal Microplate Spectrophotometer (Bio-Tek Instruments, Inc., Winooski, VT, USA).

Cell migration assays were performed using a Transwell system (Corning, NY, USA). hEM15A cells and hESCs were washed and cultured with a serum-free medium for 12 h. Next, a 100 μL aliquot of the above single-cell suspension (4×10^4 cells) was placed into the upper chambers of a Transwell plate. The lower chamber was filled with 600 μL of medium containing 15% FBS. After 48 h of incubation, a cotton swab was used to remove the cells remaining in the upper chamber. The cells that migrated into the membrane were fixed with 4% formaldehyde (Solarbio, Beijing) for 30 min and stained with 0.1% crystal violet solution (Solarbio). Eight randomly selected microscopic fields were photographed with an Eclipse Ti-s microscope (Nikon, Japan), and the number of cells in each field was counted using ImageJ software (v.1.52a).

RNA Isolation and RT-qPCR

Total RNA was isolated from MB-, FF-, and PF-derived EVs, endometrium, and cultured cells with TRIzol reagent (TaKaRa, Otsu, Japan) according to the manufacturer's instructions. The expression levels of microRNAs were evaluated by RT-qPCR using a miRNA First Strand cDNA Synthesis (Stem-loop Method) kit and microRNAs qPCR (SYBR Green Method) kit (Sangon Biotech, Shanghai, China) on an Applied Biosystems 7500 FAST instrument (Applied Biosystems, Foster City, CA, USA). For mRNA, a PrimeScript™ RT reagent Kit with gDNA Eraser (Perfect Real Time) (TaKaRa #RR047) and a QuantiNova SYBR Green PCR Kit (#208054, Qiagen, Venlo, The Netherlands) were used according to the manufacturer's instructions. All PCR primers were designed and synthesized by Sangon Biotech (Shanghai, China).

and are listed in [Supplementary Table S1](#). The detailed procedures are described in the [Supplementary Methods](#) about RNA isolation and RT-qPCR.

Western Blot Analysis

Western blot analysis were performed to quantify CD9, CD81, and Flotillin-1 protein in EVs from MB, PF, and FF, as well as ACSS2, Akt, and phospho-Akt in cells and endometrium tissues. The antibodies were CD9 (Cell Signaling Technology, Inc., Danvers, MA, USA; #13174, 1:1000), CD81 (Cell Signaling Technology; #10037, 1:1000), Flotillin-1 (Cell Signaling Technology; #18634, 1:1000), rabbit monoclonal anti-ACSS2 (Abcam, Cambridge, United Kingdom; #ab66038, 1:1000), rabbit monoclonal anti-beta Actin (Abcam; #ab8227, 1:1000), mouse monoclonal anti-GAPDH (Abcam; #ab8245, 1:1000), Akt (Cell Signaling Technology; #4691, 1:1000), Phospho-Akt (Ser473) (Cell Signaling Technology; #4060, 1:1000), goat anti-mouse IgG H&L (Abcam; #ab6789, HRP conjugated; 1:5000), and goat anti-rabbit IgG H&L antibodies (Abcam; #ab205718, HRP conjugated; 1:5000). The detailed procedures are described in the [Supplementary Methods](#) about Western blot analysis.

Immunohistochemistry and Immunofluorescence

The paraffin sections of endometrial tissue were analyzed by immunohistochemistry. hESCs from eutopic endometrial tissues were isolated and cultured as previously described, with some modifications.¹⁹ The purity of hEM15A cells and hESCs was examined using immunofluorescence staining, as described in the [Supplementary Methods](#) about immunohistochemistry and immunofluorescence.

Statistical Analysis

The relative expression levels of miRNAs in women with EM and controls were compared using the Mann–Whitney *U*-test. Spearman correlation test was used to evaluate the correlation between the validated miRNAs and the degree of symptoms. In order to estimate the association between miR-4443 levels and the presence of EM, univariable and multivariable logistic regression analyses were performed. Receiver operating characteristic (ROC) curves were generated to assess the diagnostic specificity.

All experiments were performed in triplicate. The data were expressed as means \pm standard errors of the means and were analyzed using Prism 8 (GraphPad Software Inc., San Diego, CA, USA). Differences between the two groups were evaluated using Student's *t*-test. Comparisons among three or more groups were performed by one-way analysis of variance and Tukey's post hoc test. P-values <0.05 were considered statistically significant. Statistical analyses were conducted using SPSS 25.0 for Mac (IBM Inc., Armonk, NY, USA), R 3.5.1 (R Foundation for Statistical Computing, Vienna, Austria), and Prism 8.0.1 for Mac (GraphPad Software Inc., San Diego, CA, USA).

Results

Differential Expression Profile of EV miRNAs Between EM and Non-EM Patients

EVs were extracted from MB, PF and FF by ultracentrifugation and identified by NTA (nanoparticle tracking analysis), TEM, and Western blot analysis ([Supplementary Figure S2](#)). The average diameters of MB-, PF-, and FF-derived EVs were 130.5 ± 60.4 nm, 144.9 ± 66.9 nm, and 155.9 ± 84.1 nm, respectively ([Supplementary Figure S2A](#)). EVs typically appeared to be cup-shaped and were less than 200 nm ([Supplementary Figure S2B](#)). Further validation through Western blot analysis confirmed the presence of the EV-specific markers CD9, CD81, and Flotillin-1 in isolated EVs ([Supplementary Figure S2C](#)). These results indicated that EVs were successfully isolated.

Next, we explored whether MB-derived EVs from EM patients (EM-MB-EVs) could promote proliferation and migration in hEM15A cells and primary hESCs. Firstly, in order to determine whether EM-MB-EVs could be taken up by hEM15A cells, NC-hESCs, or EM-hESCs, we labeled EVs with PKH67. Fluorescence microscopy showed the presence of green PKH67 spots in recipient cells, indicating that labeled MB-derived EVs from EM patients could be delivered into hEM15A cells, NC-hESCs, and EM-hESCs ([Supplementary Figure S3A](#)). Subsequent CCK-8 assays showed that hEM15A cells and EM-hESCs exhibited greater proliferation after taking up MB-derived EVs from EM patients compared to cells

receiving EVs from patients with benign gynecological diseases and blank controls ([Supplementary Figure S3B](#)). Moreover, Transwell chamber assays showed that hEM15A cells and EM-hESCs incubated with EM-MB-EVs exhibited increased cell migration compared to cells incubated with MB-EVs from non-EM patients ([Supplementary Figure S3C](#)). These results indicated that EM-MB-EVs could enhance the proliferation and migration of EM-ESCs.

In order to identify which EV miRNAs were expressed differently between EM and non-EM patients, we next conducted miRNA microarray analysis of MB samples (EM, n=5; non-EM, n=7), PF (EM, n=6; non-EM, n=6), and FF (EM, n=4; non-EM, n=5). A total of 202 miRNAs obtained from EM MB-derived EVs were significantly upregulated, while 221 miRNAs were downregulated, compared with their levels in the non-EM group (threshold = FC<0.8 or >1.2); 419 upregulated and 409 downregulated miRNAs were identified in EM-FF-derived EVs; and 65 upregulated and 89 downregulated miRNAs were found in EM-PF-derived EVs. Integrated analysis of the differentially expressed miRNA profiles of the MB, PF, and FF revealed eight upregulated miRNAs and 11 downregulated miRNAs that overlapped between profiles ([Figure 1A](#), see [Table 1](#) for details). The relative expression levels of the top six upregulated (ie, highest

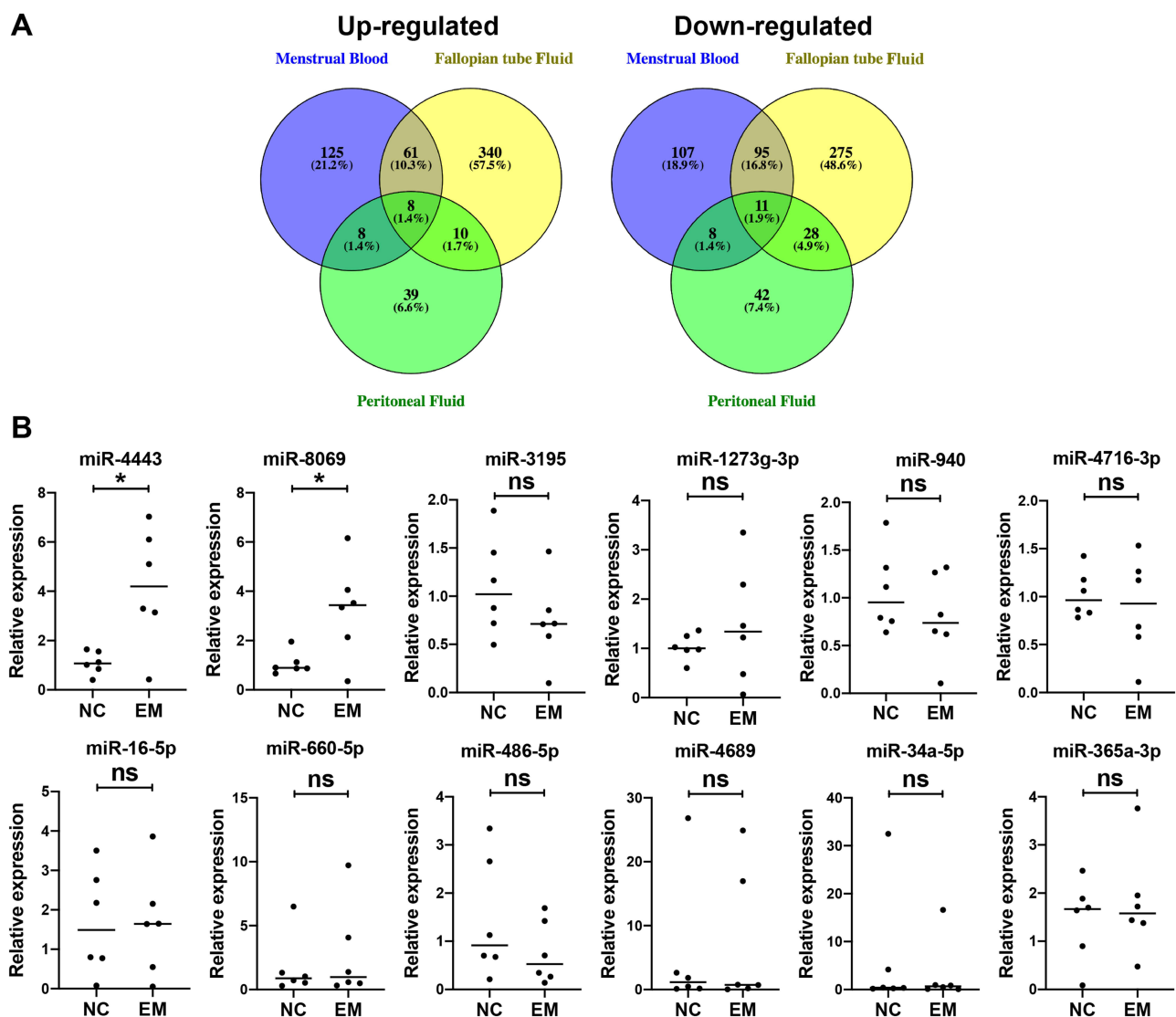


Figure 1 Agilent miRNA microarrays analysis of menstrual blood (MB)-, peritoneal fluid (PF)-, and fallopian tube fluid (FF)-derived extracellular vesicles (EVs) from endometriosis (EM) and non-EM patients and RT-qPCR confirmation of MB derived EVs-miRNAs. **(A)** Venn diagram showing the numbers of upregulated and downregulated EVs-miRNAs in MB (purple), FF (yellow), and PF (green). Eight upregulated and 11 downregulated miRNAs were the overlapping miRNAs of MB, FF, and PF samples (fold-change >1.2 or fold-change <0.8). **(B)** Relative expression levels of the top six upregulated and top six downregulated miRNAs in MB-derived EVs were confirmed by RT-qPCR assay. *P<0.05.

Abbreviation: ns, not statistically significant.

Table 1 Nineteen Overlapping EVs-miRNAs Were Statistically Different Dysregulated

Upregulated	Fold Change	P	Downregulated	Fold Change	P
hsa-miR-940	3.94	0.04	hsa-miR-198	0.80	0.62
hsa-miR-4443	3.72	0.04	hsa-miR-4419a	0.79	0.50
hsa-miR-3195	3.13	0.13	hsa-miR-1249-5p	0.75	0.35
hsa-miR-1273g-3p	2.29	0.12	hsa-miR-3610	0.71	0.67
hsa-miR-4716-3p	1.85	0.18	hsa-miR-1183	0.61	0.37
hsa-miR-8069	1.41	0.52	hsa-miR-4698	0.50	0.42
hsa-miR-3162-5p	1.31	0.46	hsa-miR-34a-5p	0.44	0.29
hsa-miR-4713-3p	1.24	0.65	hsa-miR-365a-3p	0.43	0.28
			hsa-miR-16-5p	0.29	0.18
			hsa-miR-660-5p	0.24	0.08
			hsa-miR-486-5p	0.11	0.03

FC increase) and top six downregulated (ie, highest FC decrease) MB-derived EV-miRNAs were then confirmed by qPCR relative expression analysis (Figure 1B).

miR-4443 Promoted Proliferation and Migration in hEM15A and EM-hESCs

RT-qPCR results showed that the expression of miR-4443 and miR-8069 was significantly increased in EM-MB-EVs ($P < 0.05$) (Figure 1B). Due to a complete lack of miR-8069-associated studies, miR-4443 was selected for closer scrutiny in the following experiments. The level of miR-4443 was also detected by RT-qPCR in cells co-cultured with EM-MB-EVs. Compared with cells treated with non-EM EVs or blank control EVs, hEM15A cells or hESCs co-cultured with EM-MB-EVs induced an increase in cellular levels of mature miR-4443 (all in $P < 0.05$) (Supplementary Figure S4A and C).

In order to better understand the biological role of miR-4443 in hEM15A cells and hESCs, we separately transfected both cell types with the MSCV-V26-GFP-miR-4443 retroviral overexpression vector or MSCV-V26-GFP vector control. Overexpression of miR-4443 in hEM15A cells (Supplementary Figure S4B) and hESCs (Supplementary Figure S4D) was confirmed by RT-qPCR assays. The CCK-8 assays indicated that miR-4443 overexpression led to increased proliferation of hEM15A cells ($P < 0.001$) and hESCs ($P < 0.05$) at 72 h post-transfection (Supplementary Figure S4E). Similarly, Transwell assays showed that miR-4443 upregulation resulted in significantly increased migration by hEM15A cells ($P < 0.05$) and hESCs ($P < 0.05$) cells compared with MSCV-V26-GFP vector controls (Supplementary Figure S4F). These data suggested that miR-4443 played a key role in EM-MB-EVs and enhanced the tumorigenic properties of EM and primary stromal cells.

miRNA-4443 Directly Targeted and Negatively Regulated ACSS2, Leading to the Activation of PI3K/AKT Pathway

The downstream mechanism of miR-4443 was further studied. We next sought to identify its regulatory targets using predictive bioinformatics analyses by TargetScan, miRbase, and IPA databases. These analyses revealed that ACSS2, MAPK1, CCL15, ATP6V1C2, PRSS2, CHID1, and MFAP3L were the most likely targets for interaction with miR-4443 and the effects of miR-4443 overexpression on their transcript levels were confirmed by qPCR in hEM15A cells. Overexpression of miR-4443 decreased the expression of ACSS2 and increased the expression of MAPK1 (both $P < 0.05$) (Figure 2A). ACSS2, with a more significant difference, was selected for further analysis. TargetScan analysis using miR-4443 as seed sequence revealed complementarity with positions 214–220 and 304–310 in the 3'-UTR of ACSS2 (Figure 2B). We then conducted further bioinformatic analysis to explore the potential mechanisms underlying the modulation of ACSS2 expression in hEM15A cells. Dual-luciferase reporter assays to confirm their interaction indicated that luciferase expression of the ACSS2 3'UTR construct was reduced by 14.8% in the presence of miR-4443 ($P = 0.0083$)

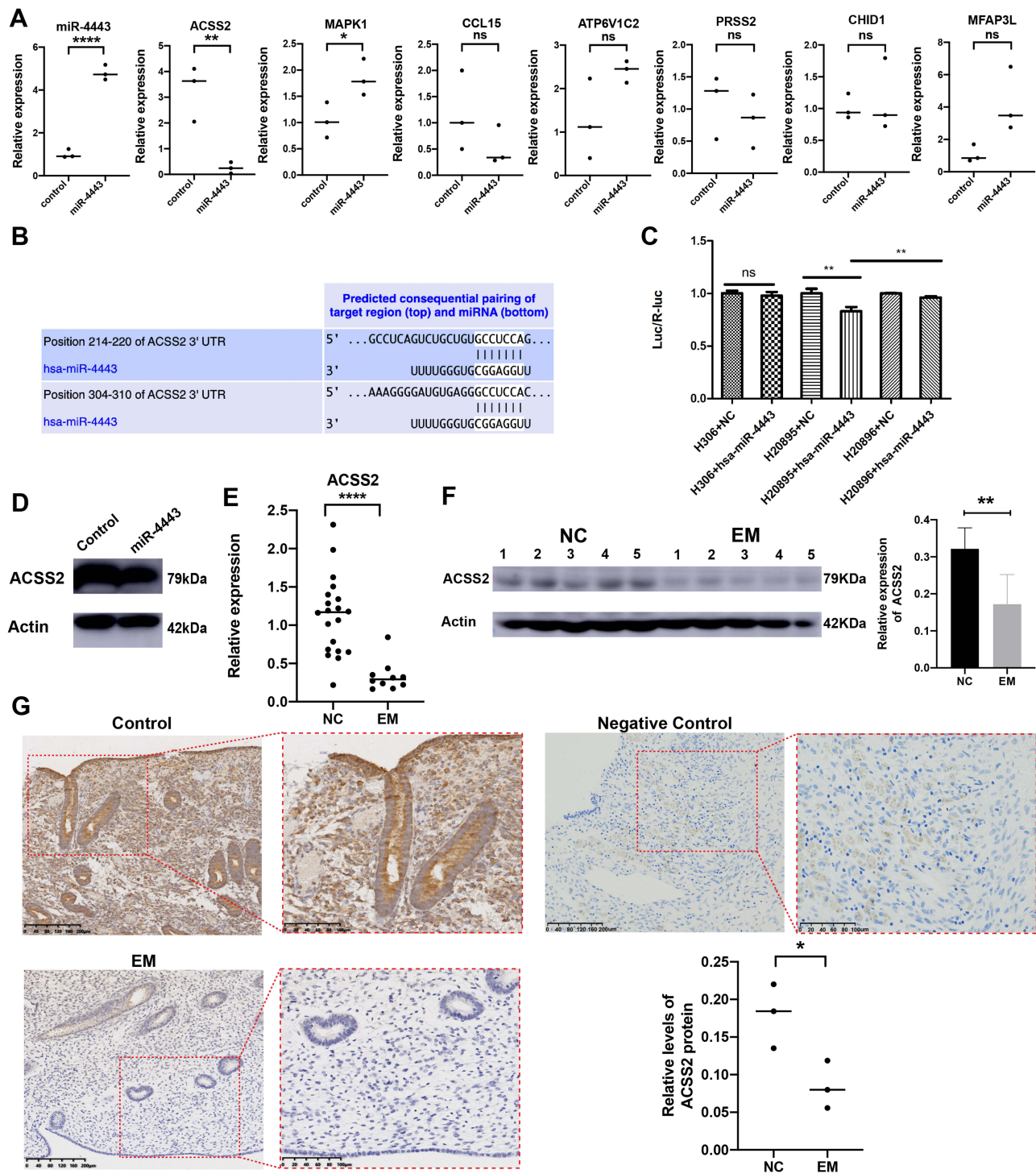


Figure 2 Screening and confirmation of the target gene of miR-4443. **(A)** RT-qPCR for the expression of miR-4443 and its predicted target genes in hEM15A cells. *P<0.05, **P<0.01, **** P<0.0001. **(B)** TargetScan results of the predicted binding sites of miR-4443 within the 3'-UTR of ACSS2 mRNA. **(C)** Dual-luciferase reporter assays to confirm the interaction between miR-4443 and the ACSS2 3'UTR. **P<0.01. **(D)** Western blot for the expression of ACSS2 in miR-4443 overexpressing retrovirus transfected hEM15A cells (miR-4443) and V26 vector retrovirus transfected hEM15A cells (Control). **(E)** RT-qPCR for the relative expression of ACSS2 in endometrium tissue from patients without endometriosis (EM) (NC, n=20) and with EM (EM, n=10). **** P<0.0001. **(F)** Western blot showing the relative protein levels of ACSS2 in endometrium tissue from patients without EM (NC, n=5) and with EM (EM, n=5). ACSS2 protein level/actin protein level had a significant difference (**P<0.01). The included samples were, from wells 1 to 5 for each group, NC-344976, NC-156370, NC-345044, NC-345032, NC-345008, EM-372301, EM-381921, EM-381924, EM-381882, and EM-379370. **(G)** Immunohistochemical analysis of the expression and localization of ACSS2 in the eutopic endometrium in patients without EM (Control, n=3), negative control, and patients with EM (EM, n=3). Scale bar=200 μm. IOD/area results of immunohistochemical analysis had a significant difference (*P<0.05). The included samples were NC-10895, NC-14167, NC-14644, EM-25791, EM-25534, and EM-26809.

Abbreviation: ns, not statistically significant.

but not with the empty vector control (Figure 2C). These results suggested that ACSS2 could serve as a target of miR-4443 and that regulatory effects were likely mediated via interaction with complementary sequences in the 3' UTR.

Next, we further explored whether miR-4443 regulated ACSS2. Western blot analysis confirmed that ACSS2 protein expression was also significantly downregulated in miR-4443-overexpression cells compared with its accumulation in control cells (Figure 2D). The RT-qPCR relative expression analysis (EM, n=10; non-EM, n=20; Figure 2E), Western blot detection (EM, n=5; non-EM, n=5; Figure 2F), and immunohistochemical staining (EM, n=3; non-EM, n=3; Figure 2G) for ACSS2 in endometrium samples from EM and non-EM patients indicated that ACSS2 was significantly downregulated in the endometrium tissue of EM patients compared with that in the non-EM control group. These findings suggested that ACSS2 expression was suppressed by miR-4443 at the transcriptional and protein level.

In order to explore the mechanism and effects of miR-4443 regulating ACSS2 on the proliferation and migration of hEM15A cells and hESCs, we silenced ACSS2 expression in hEM15A cells and hESCs. Knockdown of ACSS2 in hEM15A cells and hESCs was confirmed by qPCR analysis, which showed that ACSS2 transcript levels in the shRNA-treated cells were significantly lower than those in the control group ($P < 0.0001$; Figure 3A). We also found that ACSS2 knockdown in hEM15A cells and hESCs increased cell proliferation (Figure 3B) and cell migration (Figure 3C).

To explore the potential downstream interaction partners of ACSS2, we used mRNA sequencing (RNA-seq) analysis of ACSS2 shRNA (n=2) and control hEM15A cells (n=2) to identify genes that were differentially expressed under ACSS2 knockdown (Figure 4A and Supplementary File S1). RNA-seq data showed that suppression of ACSS2 led to significant upregulation of the PI3K/AKT signaling pathway, which was in line with our observations of enhanced proliferation and migration in ACSS2-silenced cells and the well-known effects of PI3K/AKT activation.

Transwell assays showed that exposure to LY294002 (PI3K/AKT inhibitor) inhibited the migration of hEM15A cells compared to the effects of DMSO (DMSO control) and blank control (Figure 4B). In addition, CCK-8 assays showed that LY294002 inhibited the proliferation of hEM15A cell compared with control treatments (Figure 4C). Further Western blot analysis revealed that miR-4443 overexpression or ACSS2 silencing both activated AKT signal cascade in hEM15A cells (Figure 4D), indicated by higher levels of AKT phosphorylation in endometrial tissue samples from EM patients (n=10) than in samples from non-EM patients (n=10) as well (Figure 4G). Furthermore, the addition of LY294002 to ACSS2 shRNA cells attenuated the promotion of proliferation and migration observed in untreated ACSS2-silenced cells (Figure 4E and F). Notably, treatment with LY294002 also attenuated the phosphorylation levels of AKT in ACSS2-silenced cells, while untreated ACSS2 knockdown cells exhibited a constitutive increase in AKT phosphorylation (Figure 4H). These results demonstrated that ACSS2 knockdown promoted the proliferation and migration of hEM15A cells through the activation of PI3K/AKT pathway.

miR-4443 Could Serve as a Potential Marker for EM Recurrence

Considering these findings, we quantified miR-4443 expression in MB samples from patients with EM or non-EM. No significant differences in BMI (kg/m^2) or age (years) were found between EM (EM, n=38) and non-EM (NC, n=54) patients (Supplementary Table S2). RT-qPCR assays confirmed that MB-EV miR-4443 expression was significantly higher in EM patients than in non-EM patients ($P < 0.0001$; Figure 5A). We, therefore, investigated the potential associations between miR-4443 and EM symptom severity, as judged by dysmenorrhea, dyspareunia, and gynecological history.

We found that miR-4443 levels in MB EVs were positively correlated with the degree of dyspareunia (Spearman correlation, $r=0.64$; $P < 0.0001$) and dysmenorrhea (Spearman correlation, $r=0.42$; $P < 0.01$) in the EM patients. Although not statistically significant, miR-4443 levels trended towards a negative correlation with the number of natural labors and parity in the EM patients (Figure 5B). ROC curve analyses showed an area under the curve (AUC) of 0.741 (95% CI 0.624–0.858; $P < 0.05$) for miR-4443 and an AUC of 0.929 (95% CI 0.880–0.978; $P < 0.05$) for the combination of miR-4443 and dysmenorrhea (Figure 5C).

We followed 38 patients with EM after surgery, while the remaining 21 patients declined follow-up. Patients were classified into high expression (n=19) and low expression (n=19) according to the median expression levels (0.34) of miR-4443 in MB-EVs. Kaplan-Meier survival analysis showed that EM patients with miR-4443 high expression were more likely to have a recurrence (dysmenorrhea recurrence and lesion recurrence, $P=0.0026$; Figure 5D) and were more likely to have dysmenorrhea recurrence alone, $P=0.0051$ (Figure 5E). No significant differences in lesion recurrence were

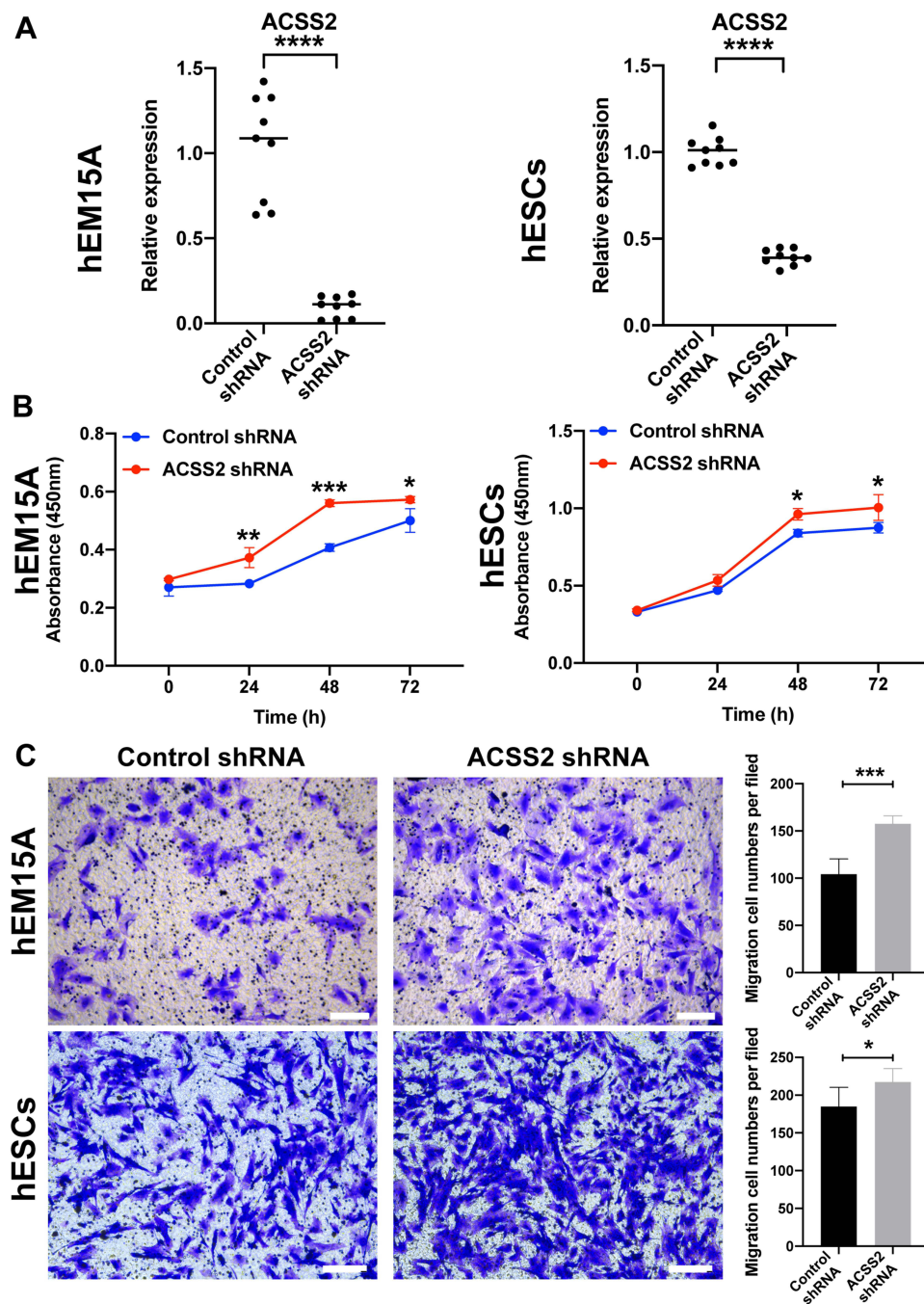


Figure 3 shACSS2 Lentivirus transfection of hEM15A and human endometrial stromal cells (hESCs) and biological function analysis. **(A)** Expression of ACSS2 in transfected hEM15A and hESCs was detected using RT-qPCR. The expression level of ACSS2 in the shACSS2 group was lower than that in the control shRNA group. **** $P < 0.0001$. **(B)** Effects of ACSS2 silencing on the proliferation of hEM15A and hESCs cells were analyzed using CCK-8 assay. The cell proliferation rate in the ACSS2 shRNA group was higher than that in the control group at different time points. * $P < 0.05$, ** $P < 0.01$, *** $P < 0.001$. **(C)** Morphology and statistical analysis of migration results showed that ACSS2 silencing promoted migration of hEM15A and hESCs cells. Scale bar=100 μm . * $P < 0.05$, *** $P < 0.001$.

detected between the miR-4443 high and low-expression patients (Figure 5F). Given these results, we proposed that miR-4443 expression levels in MB-derived EVs could serve as a candidate predictive marker for the recurrence of dysmenorrhea in EM patients (Figure 5D–F). Detailed clinical information and miR-4443 relative expression were listed in [Supplementary Table S3](#).

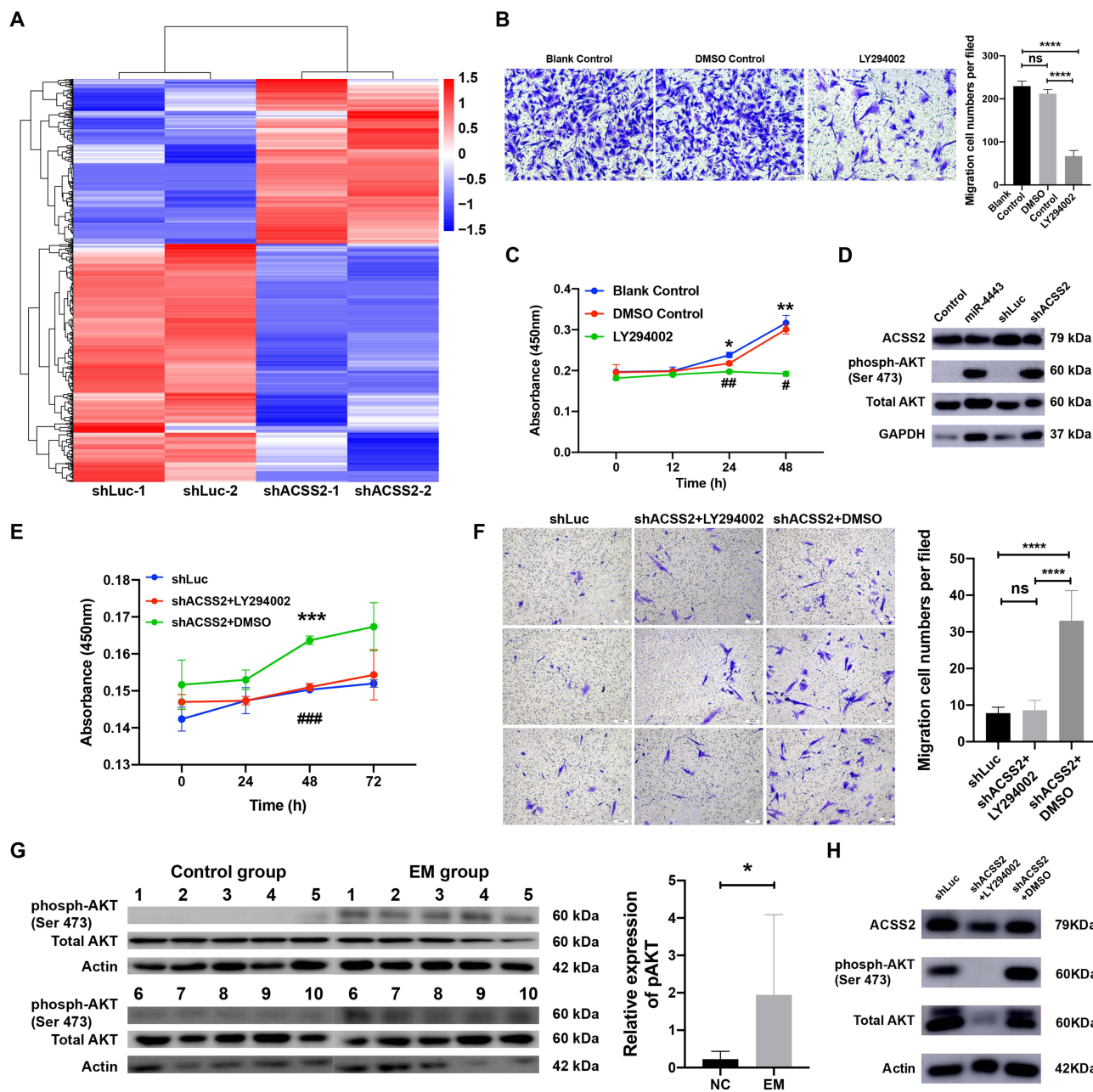


Figure 4 ACSS2 knockdown promoted the proliferation and migration of hEM15A cells via the PI3K/AKT pathway. **(A)** Heatmap of significant differentially expressed genes between shLuc (n=2) and ACSS2 shRNA transfected hEM15A cells (n=2) ($P \leq 0.05$ and $|\log_2 \text{FoldChange}| \geq 1$). **(B)** Transwell chamber assay showing that LY294002 (PI3K/AKT inhibitor) reduced hEM15A migration. Scale bar=100 μm . **** $P < 0.0001$. **(C)** The effects of the PI3K/AKT inhibitor LY294002 on the growth of hEM15A were measured by CCK-8 assay. LY294002 vs blank control: * $P < 0.05$, ** $P < 0.01$; LY294002 vs DMSO control: # $P < 0.05$, ### $P < 0.01$. **(D)** Western blot showed that overexpression of miR-4443 and silencing of ACSS2 activated AKT phosphorylation. **(E)** CCK-8 assay showed that PI3K/AKT inhibitor LY294002 rescued the growth of hEM15A induced by ACSS2 knockdown. shACSS2 +LY294002 group vs shACSS2+DMSO group: *** $P < 0.001$; shACSS2+DMSO group vs shLuc group: #### $P < 0.001$. **(F)** Transwell chamber assay showed that LY294002 rescued hEM15A migration induced by ACSS2 knockdown, Scale bar=100 μm . **** $P < 0.0001$. **(G)** p-AKT and total AKT protein levels were evaluated by Western blot in endometrium tissue from women without endometriosis (EM) (Control group, n=10) and women with EM (EM group, n=10). pAKT protein level/total AKT protein level had a significant difference (* $P < 0.05$). **(H)** Western blot showed that the elevation in the phosphorylation level of AKT following the knockdown of ACSS2 could be reversed by LY294002.

Abbreviation: ns, not statistically significant.

Discussion

EM severely decreases the patient's quality of life and increases the risk of ovarian and peritoneal cancers.^{1,2} Laparoscopy is considered to be the gold standard for EM diagnosis, but it is invasive.^{5,6} Therefore, less invasive biomarkers for EM and EM recurrence are needed. In the present study, we demonstrated that EV-encased miR-4443

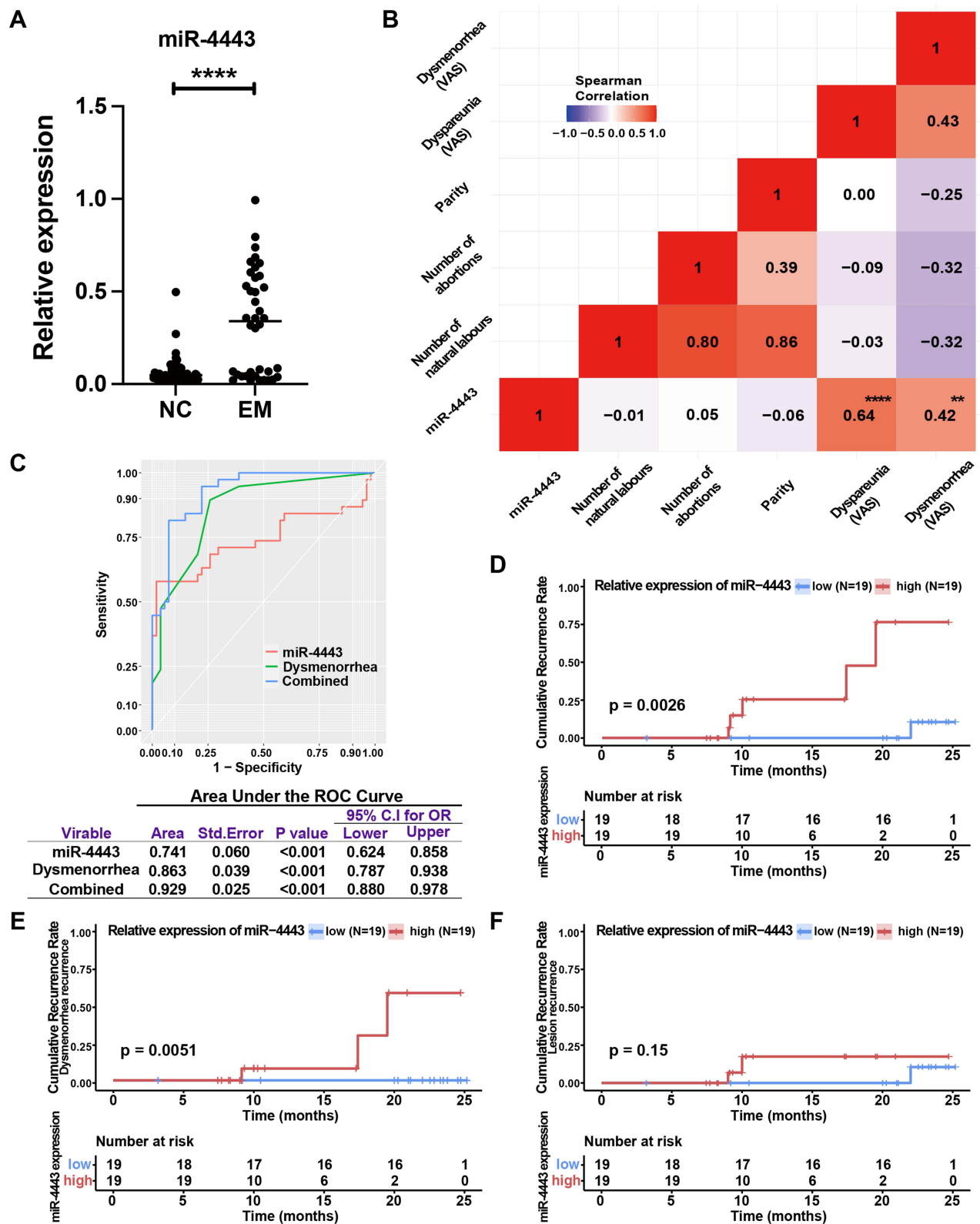


Figure 5 RT-qPCR validation and evaluation of the potential of menstrual blood (MB)-extracellular vesicles (EVs) miR-4443 serving as a biomarker for endometriosis (EM) diagnosis and recurrence. **(A)** The expression of the MB-EVs miR-4443 in patients without EM (NC, n=54) and patients with EM (EM, n=38). **** $P < 0.0001$, Mann-Whitney *U*-test. **(B)** Correlation matrix showing the Spearman correlation scores between MB-EVs miR-4443 levels and disease-related scores and reproductive history in EM samples. ** $P < 0.01$, **** $P < 0.0001$. **(C)** Receiver operating characteristic (ROC) curve showing the predictive value of MB-EVs miR-4443, dysmenorrhea, and MB-EVs miR-4443 combined with dysmenorrhea for the presence of EM. **(D)** Kaplan-Meier survival curve for cumulative recurrence rate (lesion and dysmenorrhea recurrence) of EM. **(E)** Kaplan-Meier survival curve for cumulative dysmenorrhea recurrence rate of EM. **(F)** Kaplan-Meier survival curve for cumulative lesion recurrence rate of EM.

isolated from MB could suppress ACSS2, resulting in PI3K/AKT pathway activation and promoting the migration and proliferation of ESCs. In addition, we provide strong preliminary evidence that miR-4443 levels in MB have diagnostic and predictive value for EM development and recurrence.

Firstly, our study confirmed that miR-4443 was upregulated in the MB-derived EVs from EM patients compared to non-EM patients. miR-4443 was demonstrated to be involved in the progression of breast cancer, ovarian cancer, and hepatocellular carcinoma (HCC).^{20–22} Wang et al²² showed that circulating exosomal miR-4443 might promote breast cancer cells lodging in eventual metastatic sites. Gong et al²⁰ showed that miR-4443 promoted the proliferation, migration, and invasion of HCC cells. On the other hand, Ebrahimi et al²¹ showed that a decreased expression of miR-4443 was associated with tumorigenesis and metastasis of ovarian tumors. Hence, the role of miR-4443 could be context- and tissue-dependent. miR-4443 regulates mast cells, monocytes, and T cells, and it is closely correlated with immune disorders such as Graves' disease.^{23–25} T cell-derived EVs carry miR-4443 and participate in inflammatory processes in mast cells.²⁴ In Graves' disease, miR-4443 causes T-cell dysfunction via the TRAF4 pathway.²³ Some degree of immunosuppression can be observed after a stroke, and miR-4443 plays a role in monocyte dysfunction through TRAF4.²⁵ EM is considered as a disease resulting from immune dysfunction²⁶ and chronic inflammation.²⁷ In the present study, we thus provide the first report to our knowledge of the role of miR-4443 in the pathogenesis of EM.

Furthermore, our findings revealed that miR-4443 targeted and negatively regulated ACSS2. ACSS2 is one of the genes encoding acetyl coenzyme A, a key factor in ATP production via the TCA cycle.²⁸ ACSS2 is involved in developing numerous and diverse diseases, such as gastric cancer²⁹ and glucose intolerance.³⁰ Furthermore, in HCC, ACSS2 levels are negatively correlated with the migration and invasion ability of HCC cells.³¹ In the present work, we found that the suppression of ACSS2 by the targeting of miR-4443 enhances ESC migration and proliferation, consequently promoting the progression of EM. Future studies should investigate the role of ACSS2 in EM.

Additionally, further experiments indicated that miR-4443 promotes disease progression through activation of the PI3K/AKT pathway by targeting ACSS2. The PI3K/AKT plays a pivotal role in regulating cell growth, proliferation, differentiation, and apoptosis in response to nutrient transporters and metabolic enzymes or the control of transcription factors.^{32,33} It is closely related to EM development, and its activation in the ovaries of EM patients leads to ovarian insufficiency.³⁴ In agreement with our findings, PI3K and AKT phosphorylation levels are both elevated in the eutopic endometrium of EM patients, and that inhibition of the PI3K/AKT pathway attenuates ESC migration and proliferation in EM patients.^{35,36} Nevertheless, until now, no relationship has yet been identified between ACSS2 and the PI3K/AKT signaling pathway. Here, we demonstrate that reduced ACSS2 expression can activate the PI3K/AKT signaling pathway in EM patients. It also warrants further investigation.

This study also represents the first description of miR-4443 expression, function, and potential clinical diagnostic and prognostic value in EM and provides insight into its regulatory targets and underlying pathogenic mechanisms. In particular, our results reveal that EV-encapsulated miR-4443 from MB may play a major role in the pathogenesis of EM. Moreover, this miRNA could serve as a noninvasive and simple biomarker for EM recurrence, which was verified in a larger number of patients with EM than that in previous studies, leading to greater reliability and could potentially improve diagnostic accuracy and guide postoperative treatment decisions and early intervention. Further validation in an independent and bigger patient cohort is essential for confirming our discovery.

Conclusion

Our study has elucidated that miR-4443 in EVs from MB of EM patients contributed to the pathogenesis of EM and provided insight into its regulatory targets and underlying pathogenetic mechanisms. Therefore, it could serve as a novel candidate biomarker for the noninvasive diagnosis of EM and prediction of EM recurrence. Further large-cohort studies are required to validate the diagnostic and predictive value of EV-enclosed miR-4443 in MB to improve the diagnostic accuracy and guide postoperative treatment decisions and early intervention of EM.

Abbreviations

EM, Endometriosis; miRNAs, Micro RNAs; EVs, Extracellular vesicles; MB, Menstrual blood; PF, Peritoneal fluid; FF, Fallopian tube fluid; ROC, Receiver operating characteristic; AUC, Area under the curve; CPP, Chronic pelvic pain;

hESCs, Primary human endometrial stromal cells; TEM, Transmission electron microscopy; NTA, Nanoparticle-tracking analysis; CCK-8, Cell Counting Kit-8; RNA-seq, mRNA sequencing; HCC, hepatocellular carcinoma.

Data Sharing Statement

All relevant data are available from the corresponding author upon reasonable request.

Ethics Approval and Informed Consent

This study was approved by the institutional ethics committee of the International Peace Maternity and Child Health Hospital in Shanghai, China (No. GKLW-2016-42). Written informed consent was obtained from the participants before enrollment. Our study complies with the Declaration of Helsinki.

Acknowledgments

We thank Dr. Zhao-Bo Lin and Dr. Zhen-Wu Zhang from the School of Life Science and Technology, Shanghai Tech University, for their technical assistance. The graphic abstract was created with BioRender.com.

Author Contributions

All authors made a significant contribution to the work reported, whether that is in the conception, study design, execution, acquisition of data, analysis and interpretation, or in all these areas; took part in drafting, revising or critically reviewing the article; gave final approval of the version to be published; have agreed on the journal to which the article has been submitted; and agree to be accountable for all aspects of the work.

Funding

This work was supported by the Shanghai Municipal Key Clinical Specialty, Shanghai, China (shslczdzk01802), the Clinical Science and Technology Innovation Program from Shanghai Shenkang Hospital Development Center (SHDC12019113), and the National Key Research and Development Program (2018YFC1002102).

Disclosure

The authors declare no conflict of interest in this work.

References

1. Giudice LC, Kao LC. Endometriosis. *Lancet*. 2004;364(9447):1789–1799. doi:10.1016/S0140-6736(04)17403-5
2. Hickey M, Ballard K, Farquhar C. Endometriosis. *BMJ*. 2014;348(5):g1752. doi:10.1136/bmj.g1752
3. Škegro B, Bjedov S, Mikuš M, et al. Endometriosis, pain and mental health. *Psychiatry Danub*. 2021;33(Suppl 4):632–636.
4. Mikuš M, Matak L, Vujić G, et al. The short form endometriosis health profile questionnaire (EHP-5): psychometric validity assessment of a Croatian version. *Arch Gynecol Obstet*. 2023;307(1):87–92. doi:10.1007/s00404-022-06691-1
5. Dunselman GA, Vermeulen N, Becker C, et al. ESHRE guideline: management of women with endometriosis. *Hum Reprod*. 2014;29(3):400–412. doi:10.1093/humrep/det457
6. Rimbach S, Ulrich U, Schweppe KW. Surgical therapy of endometriosis: challenges and controversies. *Geburtshilfe Frauenheilkd*. 2013;73(9):918–923. doi:10.1055/s-0033-1350890
7. Burney RO, Giudice LC. Pathogenesis and pathophysiology of endometriosis. *Fertil Steril*. 2012;98(3):511–519. doi:10.1016/j.fertnstert.2012.06.029
8. McKinnon B, Mueller M, Montgomery G. Progesterone resistance in endometriosis: an acquired property? *Trends Endocrinol Metab*. 2018;29(8):535–548. doi:10.1016/j.tem.2018.05.006
9. Busacca M, Chiaffarino F, Candiani M, et al. Determinants of long-term clinically detected recurrence rates of deep, ovarian, and pelvic endometriosis. *Am J Obstet Gynecol*. 2006;195(2):426–432. doi:10.1016/j.ajog.2006.01.078
10. Guo SW. Recurrence of endometriosis and its control. *Hum Reprod Update*. 2009;15(4):441–461. doi:10.1093/humupd/dmp007
11. Shimizu K, Kamada Y, Sakamoto A, Matsuda M, Nakatsuka M, Hiramatsu Y. High expression of high-mobility group box 1 in menstrual blood: implications for endometriosis. *Reprod Sci*. 2017;24(11):1532–1537. doi:10.1177/1933719117692042
12. Chen Y, Wang K, Xu Y, et al. Alteration of myeloid-derived suppressor cells, chronic inflammatory cytokines, and exosomal miRNA contribute to the peritoneal immune disorder of patients with endometriosis. *Reprod Sci*. 2019;26(8):1130–1138. doi:10.1177/1933719118808923
13. Colombo M, Raposo G, Thery C. Biogenesis, secretion, and intercellular interactions of exosomes and other extracellular vesicles. *Annu Rev Cell Dev Biol*. 2014;30(1):255–289. doi:10.1146/annurev-cellbio-101512-122326
14. Fassbender A, Burney RO, Df O, D’Hooghe T, Giudice L. Update on biomarkers for the detection of endometriosis. *Biomed Res Int*. 2015;2015:130854. doi:10.1155/2015/130854

15. Gupta D, Hull ML, Fraser I, et al. Endometrial biomarkers for the non-invasive diagnosis of endometriosis. *Cochrane Database Syst Rev.* 2016;4(4):CD012165. doi:10.1002/14651858.CD012165
16. Warren LA, Shih A, Renteira SM, et al. Analysis of menstrual effluent: diagnostic potential for endometriosis. *Mol Med.* 2018;24(1):1. doi:10.1186/s10020-018-0009-6
17. Khalaj K, Miller JE, Lingegowda H, et al. Extracellular vesicles from endometriosis patients are characterized by a unique miRNA-lncRNA signature. *JCI Insight.* 2019;4(18). doi:10.1172/jci.insight.128846
18. Brennan K, Martin K, FitzGerald SP, et al. A comparison of methods for the isolation and separation of extracellular vesicles from protein and lipid particles in human serum. *Sci Rep.* 2020;10(1):1039. doi:10.1038/s41598-020-57497-7
19. Zhang C, Large MJ, Duggavathi R, et al. Liver receptor homolog-1 is essential for pregnancy. *Nat Med.* 2013;19(8):1061–1066. doi:10.1038/nm.3192
20. Gong J, Wang J, Liu T, Hu J, Zheng J. lncRNA FEZF1AS1 contributes to cell proliferation, migration and invasion by sponging miR4443 in hepatocellular carcinoma. *Mol Med Rep.* 2018;18(6):5614–5620. doi:10.3892/mmr.2018.9585
21. Ebrahimi SO, Reisi S. Downregulation of miR-4443 and miR-5195-3p in ovarian cancer tissue contributes to metastasis and tumorigenesis. *Arch Gynecol Obstet.* 2019;299(5):1453–1458. doi:10.1007/s00404-019-05107-x
22. Wang J, Zhang Q, Wang D, et al. Microenvironment-induced TIMP2 loss by cancer-secreted exosomal miR-4443 promotes liver metastasis of breast cancer. *J Cell Physiol.* 2020;235(7–8):5722–5735. doi:10.1002/jcp.29507
23. Qi Y, Zhou Y, Chen X, et al. MicroRNA-4443 causes CD4+ T cells dysfunction by targeting TNFR-associated factor 4 in Graves' disease. *Front Immunol.* 2017;8:1440. doi:10.3389/fimmu.2017.01440
24. Shefler I, Salamon P, Levi-Schaffer F, Mor A, Hershko AY, Mekori YA. MicroRNA-4443 regulates mast cell activation by T cell-derived microvesicles. *J Allergy Clin Immunol.* 2018;141(6):2132–2141 e2134. doi:10.1016/j.jaci.2017.06.045
25. Li S, Lu G, Wang D, et al. MicroRNA-4443 regulates monocyte activation by targeting tumor necrosis factor receptor associated factor 4 in stroke-induced immunosuppression. *Eur J Neurol.* 2020;27(8):1625–1637. doi:10.1111/ene.14282
26. Symons LK, Miller JE, Kay VR, et al. The immunopathophysiology of endometriosis. *Trends Mol Med.* 2018;24(9):748–762. doi:10.1016/j.molmed.2018.07.004
27. Mikuš M, Goldštajn M, Brlečić I, et al. CTLA4-linked autoimmunity in the pathogenesis of endometriosis and related infertility: a systematic review. *Int J Mol Sci.* 2022;23(18):10902. doi:10.3390/ijms231810902
28. Comerford SA, Huang Z, Du X, et al. Acetate dependence of tumors. *Cell.* 2014;159(7):1591–1602. doi:10.1016/j.cell.2014.11.020
29. Hur H, Kim YB, Ham IH, Lee D. Loss of ACSS2 expression predicts poor prognosis in patients with gastric cancer. *J Surg Oncol.* 2015;112(6):585–591. doi:10.1002/jso.24043
30. Wopereis S, Radonjic M, Rubingh C, et al. Identification of prognostic and diagnostic biomarkers of glucose intolerance in ApoE3Leiden mice. *Physiol Genomics.* 2012;44(5):293–304. doi:10.1152/physiolgenomics.00072.2011
31. Sun L, Kong Y, Cao M, et al. Decreased expression of acetyl-CoA synthase 2 promotes metastasis and predicts poor prognosis in hepatocellular carcinoma. *Cancer Sci.* 2017;108(7):1338–1346. doi:10.1111/cas.13252
32. Hennessy BT, Smith DL, Ram PT, Lu Y, Mills GB. Exploiting the PI3K/AKT pathway for cancer drug discovery. *Nat Rev Drug Discov.* 2005;4(12):988–1004. doi:10.1038/nrd1902
33. Hoxhaj G, Manning BD. The PI3K-AKT network at the interface of oncogenic signalling and cancer metabolism. *Nat Rev Cancer.* 2020;20(2):74–88. doi:10.1038/s41568-019-0216-7
34. Takeuchi A, Koga K, Satake E, et al. Endometriosis triggers excessive activation of primordial follicles via PI3K-PTEN-Akt-Foxo3 pathway. *J Clin Endocrinol Metab.* 2019;104(11):5547–5554. doi:10.1210/jc.2019-00281
35. Madanes D, Bilotas MA, Baston JI, et al. PI3K/AKT pathway is altered in the endometriosis patient's endometrium and presents differences according to severity stage. *Gynecol Endocrinol.* 2020;36(5):436–440. doi:10.1080/09513590.2019.1680627
36. Wang H, Ni C, Xiao W, Wang S. Role of lncRNA FTX in invasion, metastasis, and epithelial-mesenchymal transition of endometrial stromal cells caused by endometriosis by regulating the PI3K/Akt signaling pathway. *Ann Transl Med.* 2020;8(22):1504. doi:10.21037/atm-20-6810